

OPTICAL STUDIES OF COLORED CHEMICAL SPECIES

M.R. Behfroz

Department of Physics, University of Urumia, Urumia, Islamic Republic of Iran

Abstract

Evanescent wave spectroscopy using thin optically transparent electrodes and multiple reflections allows unique observations of the electrochemical interphase since the region of solution sampled is typically 100 nm from the electrode in the visible spectral region. This technique is found to be highly sensitive to the presence of absorbing adsorbed species.

Introduction

Throughout the history of modern physics and chemistry, probably the greatest experimental contribution to the development of quantum mechanics and atomic and molecular structure has been spectroscopy. Its application is in general limited to the homogeneous gas, liquid, and solid states. Direct spectroscopic observation of individual surface species is beyond the scope of conventional spectroscopy. However, the elusive interphase region of surface science, which is the heart of electrochemistry, the focal point of most biological functions, and the site of heterogeneous catalysis, can be sensitively probed by EWSF (evanescent wave spectroscopy in the presence of thin metallic film) thus facilitating the study of surface species without complications from an absorbing final phase. An optically transparent thin metal film electrode as part of an EWSF cell allows spectroscopic and electrochemical observations to take place simultaneously during potential modulations.

Techniques and methods are presented in this paper which illustrate the powerful EWSF approach in determining surface coverage, adsorption-desorption rates, and concentration changes at the electrode-electrolyte interface. Electronic absorption occurs in the UV for most chemical species of interest. However, crystal violet (CV) and methylene blue (MB) exhibit distinct electronic absorption in the visible and both specifically adsorb. Since the principle of electronic absorption is the same in the UV and visible, the discussions presented here are equally

applicable to the study of species in the UV.

Theoretical Considerations

An electromagnetic wave striking the interface at an angle greater than the critical angle ($n_1 > n_2$) penetrates the final phase to penetration depth d , which for 72.7° on glass-water interface is only $.14\lambda_0$, hence, absorbing adsorbed layers will dominate the EWS spectra. In fact, for parallel polarization at this angle of incidence, the ratio of EWS absorbance due to solution to transmittance is $.8\lambda_0/b$ where the concentration is the same for each case, λ_0 is the wavelength *in vacuo*, and b is the thickness of the transmission cell. For a non-adsorbed absorbing species at 530 nm with $b = .01$ cm, transmission and EWS absorbances are equivalent when the concentration behind the EWS plate is approximately 235 times that in the transmission cell. For a precise comparison, the anomalous dispersion of the final phase with changing concentration of absorbing species and the dependence on wavelength for EWS spectra must be taken into consideration. However, any EWS absorbance for dilute solutions will be due only to adsorbed layers since the solution contribution would be negligible for concentrations of CV less than .3 mM under normal conditions.

The absorbance per reflection of an adsorbing species can be described for EWS by the expression (1)

$$A/N = a_{ad} h_{eff} c_{ad} S + ab_{off} c S + ab_{off} c (1-S) \quad (1)$$

where

Keywords: Optics; Physical chemistry; Surface physics

A= absorbance measured
 N= the number of reflections
 a_{ad} = molar absorptivity of adsorbed species
 h_{eff} = effective thickness of adsorbed layer of actual thickness h
 c_{ad} = concentration of adsorbed species
 S= surface coverage of adsorbed layer
 a= molar absorptivity of absorbing species in solution
 c= concentration of species in solution
 b_{eff} = effective thickness of EWSF cell, or the thickness of a transmission cell required to give an equivalent absorbance

The first term on the right side of the equal sign is the absorbance contribution of the partial adsorbed layer, the second term is the contribution of bulk solution, and the third term compensates for that part of the surface not yet adsorbed onto. The value S equals unity when A has reached an equilibrium value representing the absorbance for the adsorption of a complete monolayer. A sensitivity factor dependent on optical parameters appears in the effective thickness terms such that $h_{eff} = \beta h$ and $b_{eff} = \beta d$ where h is the actual thickness of the adsorbed layer and d is the penetration depth as previously discussed. A theoretical calculation [1] yields this sensitivity factor to be

$$\beta = \frac{n_2}{n_1 \cos \theta} \frac{\langle E^2 \rangle_2}{\langle E^2 \rangle_1} \quad (2)$$

where θ is the angle of incidence, n the index of the semi infinite final phase for b_{eff} or of the adsorbed layer for h, $\langle E^2 \rangle_2$ is the time average of the E field squared at the interface, or for a thin film, the space time average inside the film, and $\langle E^2 \rangle_1$ is the time average in phase 1. The fields are taken at the glass-solution interface with no adsorption in calculating b_{eff} in equation (1), while b_{eff} incorporates the fields at the thin film-solution interface. A thin film may markedly change the fields sampling the solution which is reflected in the sensitivity factor. Calculations for the E fields at the interface are exact thus enabling precise determination of β .

For concentrated solutions, in which the solution contribution to the absorbance is indeed appreciable and S has had sufficient time to reach unity, equation (1) is linear in c provided the molar absorptivity is constant. Extrapolation to $c=0$ gives the absorbance of the adsorbed monolayer A_{ad} . This can be expressed as

$$A_{ad} = a_{ad} h_{eff} c_{ad} = 1000 a_{ad} \beta \Gamma_{ad} \quad (3)$$

where Γ_{ad} is the surface concentration in mole-cm⁻². The 1000 factor converts volume concentration in liters to cm³.

With a knowledge of the optical constants of the adsorbed monolayer, the surface concentration is easily determined. The effective optical constants can be determined from values of A_{ad} obtained under different experimental conditions such as absorbance measurements at $\theta=72^\circ$ for each polarization and a transmission measurement at normal incidence [2].

Internal reflection measurements in the presence of intermediate thin metal films differ from the no film case. This effect is taken into account in the b_{eff} term. The optical constants of the intermediate films enable determination of $\langle E^2 \rangle$ in β , which will now be taken at the metal-solution interface, and n_2 , instead of being the index of phase two, is the index of the semi-infinite final phase with no adsorption.

For the present case of a single metal film, a 60Å gold evaporated film on glass, $n = .816$, $K=2.228$ at 530 nm and $n = .46$, $K=3.20$ at 605 nm resulting in b_{eff} being 583 nm and 690 nm respectively for parallel polarization and 112 nm and 144 nm for perpendicular polarization maintaining the final phase as H₂O. Extrapolation to $c=0$ for EWSF absorbance-concentration plots will yield further information about adsorbed monolayers. Any deviations in EWS and EWSF observed monolayers will be readily apparent.

Crystal violet and methylene blue are both known to specifically adsorb [4]. Adsorbed molecules can, in general, be potentiostatically desorbed from a gold electrode. The accomplishment of this, however, will depend on how large the potential barrier associated with the adsorption mechanism is, i.e. will the potential barrier be overcome prior to the occurrence of the reduction or oxidation process. The addition of ethanol into the electrolyte reduces the adsorption bonding of these dyes enabling them to "come and go" as a function of potential without redox systems interfering. For a particular electrolytic solution, adsorption occurs at definite potentials allowing this process to be observed spectroscopically as a function of potential. In addition to varying the potential linearly and observing the resultant absorbance, the potential can be stepped from a region where no adsorption occurs to where the dyes do absorb. The frequency of the potential step which limits the total absorbance change to that determined by the extrapolation procedure, i.e. S equals unity, defines the adsorption rate constant. The rate will depend on concentration and can be expressed by

$$\frac{d\Gamma_{ad}}{dt} = K_{ad} c \quad (4)$$

where Γ_{ad} is as previously defined and is proportional to the absorbance measured, c is the concentration in solution, and K_{ad} is the constant to be determined. The desorption rate constant is defined similarly but should be independent

dent of solution concentration yet will depend on the amount adsorbed. Thus,

$$\frac{d\Gamma_{ad}}{dt} = K_{des} c_{ad} = K_{des} \frac{1000 \beta \Gamma_{ad}}{h_{eff}} \quad (5)$$

where K_{des} is the desorption rate constant. The time interval is the time for the absorbance to decrease from A_{ad} to zero. All other quantities in (5) are determined separately allowing K_{des} to be calculated.

Experimental Section

Multiple internal reflection units were used for reflection measurements and consisted of two prism arrange-

ments in optical contact with the glass plate of an EWSF cell which is depicted in Figure 1. The plate, when coated with a thin metal film, served as the working electrode in the electrochemical cell. The entrance and exit prisms define the angle of incidence θ at the plate-solution interface such that

$$\theta = \psi + \sin^{-1} \frac{\cos \psi}{n_1} \quad (6)$$

where ψ is the prism angle, as shown in part b of Figure 1, and n_1 is the index of the glass plate and prisms. The window width indicates the maximum allowable beam width [3] and is given by

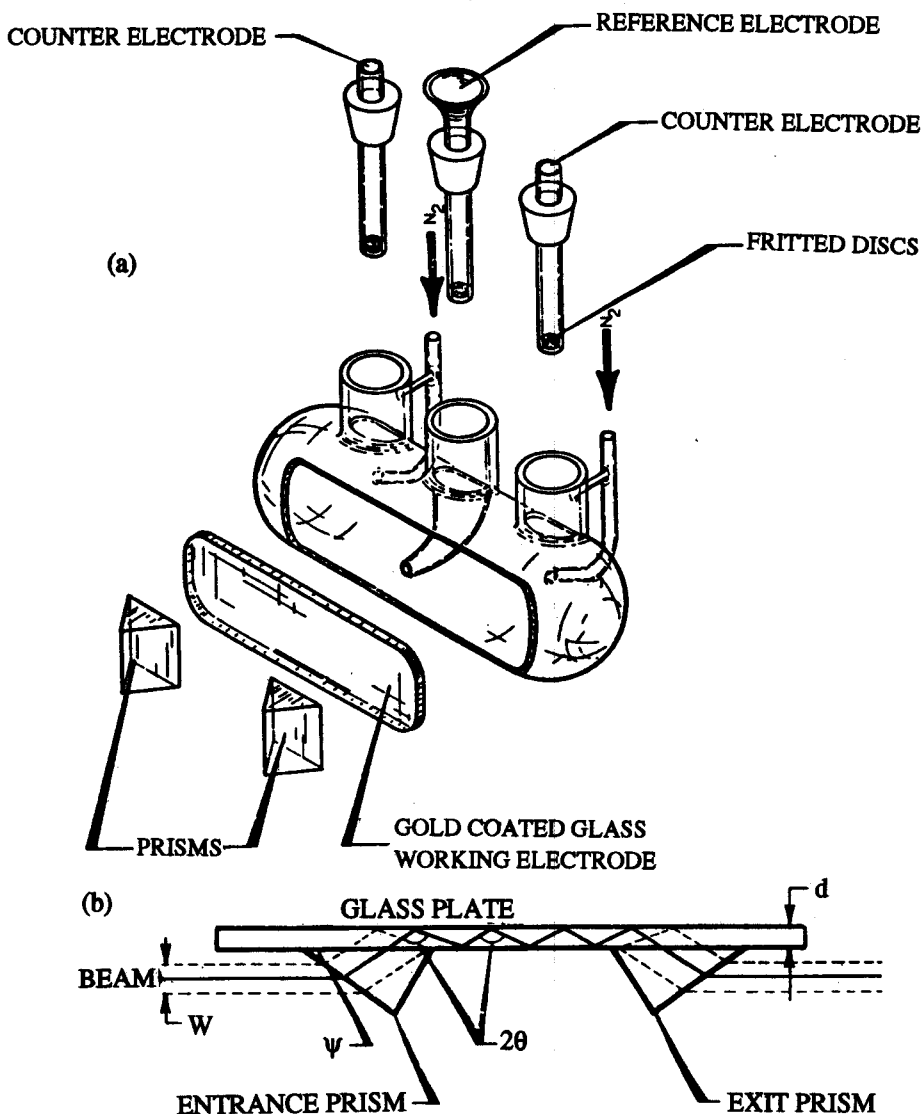


Figure 1. The electrochemical cell (a) and a typical internal reflection arrangement (b) for EWS and EWSF observations.

$$W = \frac{2d}{1 + \cot \theta \cot \psi} \quad (7)$$

where d is the thickness of the plate. A 72° reflection unit was used in this study to insure that the incident beam was beyond the critical angle for the glass-electrolyte system. Transmission cells of various thicknesses were used for transmission absorbance measurements. All reflection and transmission units were made to fit a Cary Model 14 Recording Spectrophotometer with expanded sample compartment. The visible light source was a quartz-iodide lamp operating at a black body temperature of 3500°K with a usable range from 320 to 700 nm.

Triply deionized water was used throughout the investigation. Crystal violet (CV) [4], of medicinal purity, was recrystallized while methylene blue (MB) and Eosin B were not further purified. All chemicals for supporting electrolyte were reagent grade. Solution temperatures were allowed to equilibrate to room temperature at $23 \pm 1^\circ\text{C}$ for potential measurements. All potentials are reported with respect to the aqueous saturated calomel electrode (SCE). Bottled nitrogen was additionally purified by passing through a wash tower containing a chromous sulfate solution prior to deaerating the electrolytic solutions.

Gold was vacuum evaporated on high quality fire polished microscope slides and float glass of various thicknesses. The 60 \AA gold film resistances of $20 \text{ } \Omega/\text{sq}$ were reduced to $15 \text{ } \Omega/\text{sq}$ after cleaning in sodium nitrate at 330°C and rinsing in deionized H_2O . The float glass gold films turned pale blue if left in the bath for more than a few seconds. The films adhered better to the slides and were stable for more than 20 seconds exposure time in the nitrate solution. Electrical contact to the gold film was made through silver epoxy and silver conducting paint completely surrounding the solution interface of the working electrode but not in contact with the electrolyte. The EWSF cell, with a working electrode area of 8.4 cm^2 , was sealed to maintain an inert atmosphere of oxygen free nitrogen.

Crystal violet and methylene blue were two species chosen since both are known to specifically adsorb. Eosin B, conversely, does not adsorb and was used where adsorption was not desired. The adsorbing dyes were first studied optically and then potentiostatically using the dropping mercury electrode, a bulk gold electrode, and then the thin film gold electrode since the thin film approximates the bulk gold and allows for spectroscopic observations during potential modulations.

Results and Discussion

Optical Characterization of Colored Species

Figures 2 and 3 are plots of the absorptivities for CV and MB as calculated from transmission measurements for

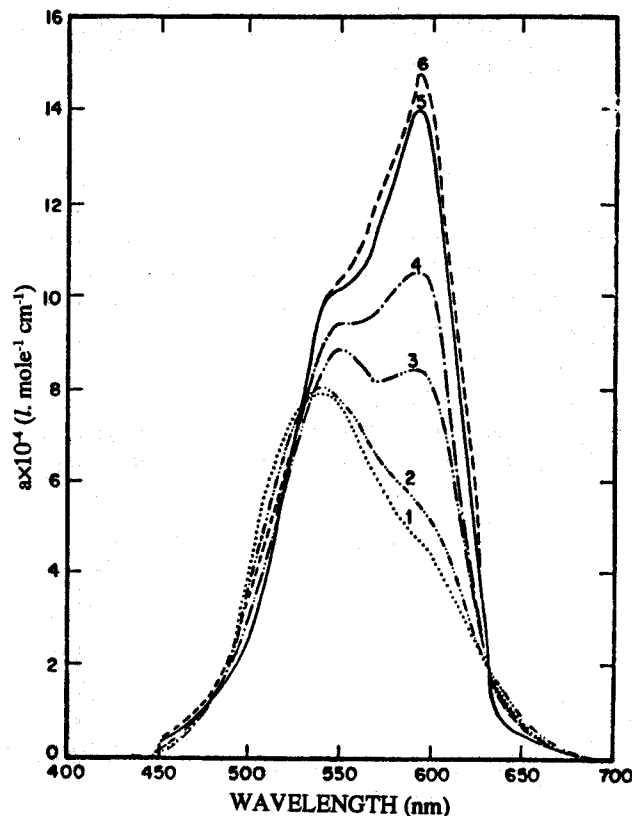


Figure 2. Absorptivities of crystal violet in H_2O . Concentrations are (1) 6.0 mM, (2) 3.0 mM, (3) .60 mM, (4) .30 mM, (5) 6.0 μM , and (6) 3.0 μM .

various concentrations. Deionized H_2O is the solvent for the CV curves shown while MB is in a phosphate buffer solution with a pH of 7.4. The transmission characteristics discussed here for each dye remain unaffected when the solvents are interchanged. Each of the spectra appears to be made up of two bands: a monomer band peaking at 590 nm for CV and 665 nm for MB, and a polymer band with a maximum at 540 nm for CV and 605 nm for MB. The polymer bands are prominent at higher concentrations while the monomer dominates at lower concentrations. The CV bands are roughly equivalent near .6 mM concentrations while the changeover for MB occurs lower at .1 mM. This indicates that MB polymerizes more readily than CV does in solution.

Figure 4 discloses the enhanced monomer band with addition of ethanol to a 12.5 micromolar solution of MB. The percentage indicates the ratio of ethanol by volume to total solution. For 1.25 mM concentration of MB, a 20% ethanol mixture increases the monomer band to that of the polymer band and for a 50% mixture, the absorptivity appears similar to the 6.25 mM curve in Figure 3. The monomers tend to polymerize in concentrated aqueous solution but the polymerized forms are much more soluble

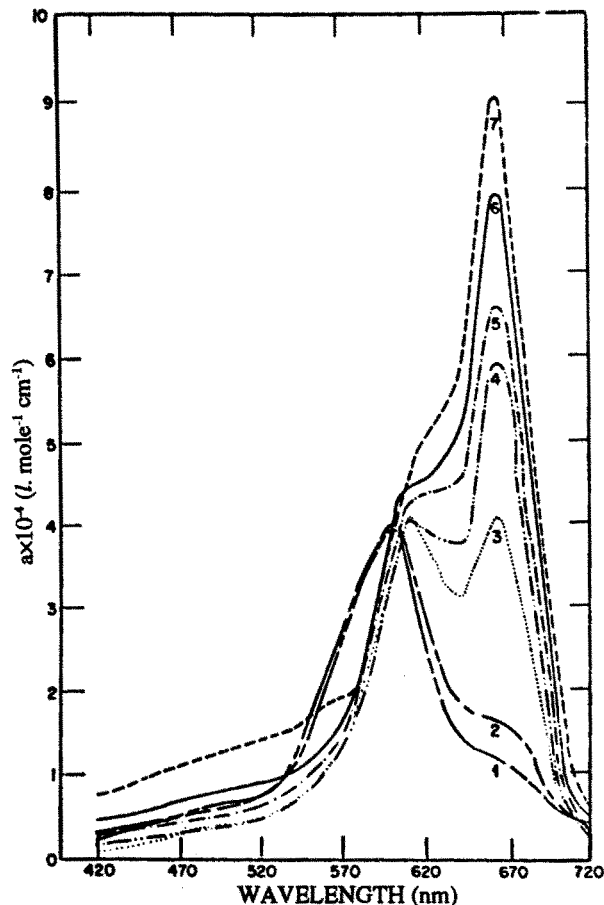


Figure 3. Absorptivities of methylene blue in phosphate buffer with a pH of 7.4. Dye concentrations are (1) 10 mM, (2) 2.5 mM, (3) 1.0 mM, (4) 50 μM, (5) 25 μM, (6) 12.5 μM, and (7) 6.25 μM.

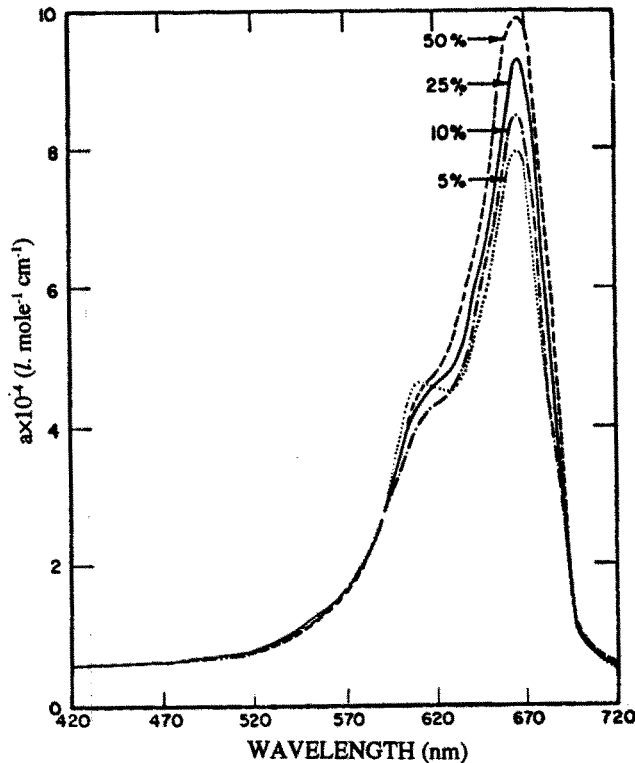


Figure 4. Absorptivities of 12.5 μM methylene blue in phosphate buffer. The percentage of ethanol by volume to total solution is varied from 5 to 50%.

ethanol solution and disassociate to the monomer form. In a similar manner, ethanol mixtures reduce the polymer and of CV and enhance the monomer band. The linearity of absorbance with concentration is a requisite for calculations and analysis presented later and these two points roughly satisfy that requirement. Part of the non linearity, especially for dilute solutions, is due to adsorption since absorbance contribution can become increasingly large as the concentration in solution decreases.

Dilute CV solutions were monitored by EWS as the concentration was gradually increased in increments to observe information about a CV adsorbed layer. A well defined monolayer would give a plateau in absorbance-concentration plots provided the adsorbed layer consisted of a single layer of CV molecules or, if micelles constituted the layer, the aggregate number per micelle was a constant. However, the resulting absorbance measurements gradually increased with time and concentration. Although the slope decreased with increasing concentration, no plateau resulted. This indicates that an adsorbed layer does not

form instantly but is a function of concentration and also that aggregate numbers higher than unity constitute the adsorbed layer. Additional time and concentration allow higher aggregates to form which in turn increases the concentration of dye molecules near the surface sampled by EWS resulting in increased absorbance. MB behaves in a similar manner but to a lesser degree than CV.

Absorbance concentration curves for adsorbing CV are compared to non-adsorbing Eosin B in Figure 5 to test the extrapolation procedure of determining an adsorbed layer. The measurements for CV were taken at 530 nm and 512 nm for Eosin B. The curves are the result of least squares fits to the data. The relative concentrations differ for curves 4-7 to indicate the independence of A_{ad} on absolute concentration and time of measurement.

Eosin B intercepts the axis where expected (curves 1 and 2) but CV intercepts in two separate areas for parallel polarization. The intercepts at .095 were obtained using an ATR plate of float glass whereas the lower ones correspond to fire polished microscope slides. Further investigation resolved the discrepancy.

After the spectrum of a concentrated solution of CV on float glass was obtained, the cell was carefully rinsed several times until no color remained in the solution. The

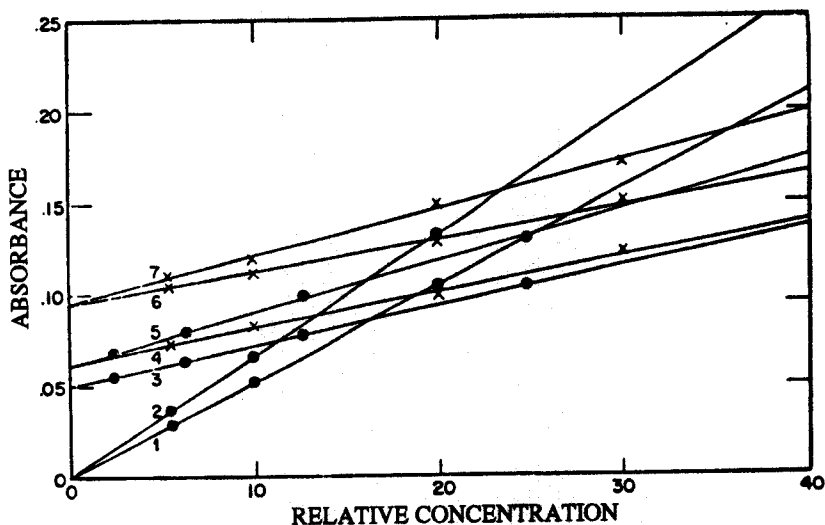


Figure 5. EWS absorbance-concentration behavior per reflection at 72° for various solutions. Conditions are (1) 5 gm of Eosin B per liter of pH 7.4 phosphate buffer, $\lambda = 512$ nm, and \perp Polarization, (2) same as (1) except \parallel polarization, (3) .9 mM CV, $\lambda = 540$ nm, and \perp polarization, (4) .5 mM CV and \parallel polarization, (5) .9 mM CV and \parallel polarization, (6) .5 mM CV and \parallel polarization but using float glass instead of microscope slide, and (7) same as (6) except .9 mM CV. All concentrations correspond to a relative concentration of 1.0.

spectrum of the remaining adsorbed layer was obtained after which the cell was completely cleaned and the above procedure repeated with a different concentration. Figure 6 discloses the results of this experiment. The resulting spectrum is highly reproducible and at 530 nm, the absorbance is roughly the same as the A vs c intercept using the microscope slide. After several trials, the A_{ad} by intercepts to A_{ad} by rinsing ratio is consistently 1.48 indicating that CV adsorbs on the float glass in a reproducible fashion in addition to a prescribed amount being removed by rinsing. The float glass evidently has a different type surface which allows a semi-mobile layer of CV to be lightly bound and which is easily washed off. Rinsing the adsorbed layer on the slides yields a negligible change in absorbance. The shape of the resulting spectrum in Figure 6 indicates that the adsorbed layer consists of polymers rather than monomers.

The surface coverage decreases as the percentage of alcohol increases until at 50%, S goes to zero. This percentage of ethanol makes the previously insoluble adsorbed layer dissolve into the solution and also prevents further adsorption under normal conditions.

Extrapolation to $c = 0$ for transmission measurements will also give information about the adsorbed layer, however, transmission absorbance due to this layer will be very small. For $S = 1$ transmission absorbance to a first approximation is $A = 2a_{ad}hc_{ad} + a(b-2h)c$ where b is the cell thickness and the factor of 2 appears since there are two

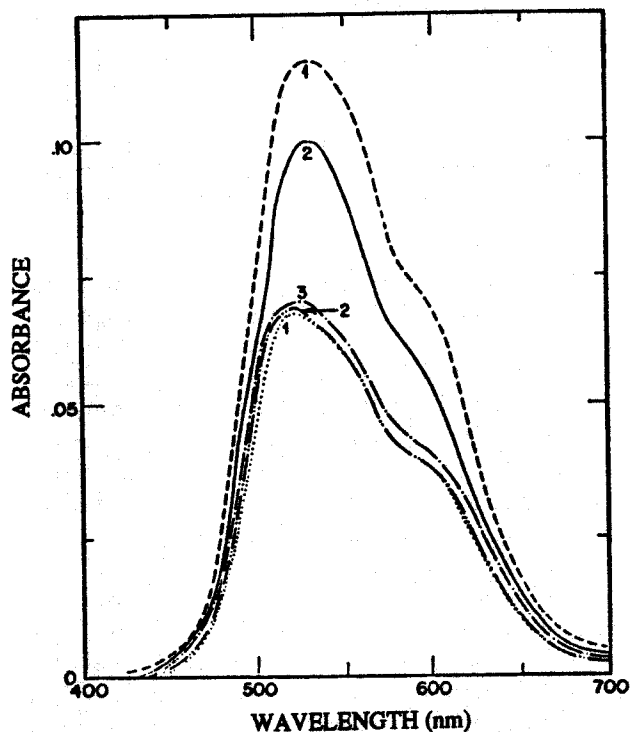


Figure 6. EWS absorbance spectra of crystal violet in H_2O at 72° using float glass plate before and after rinsing. Concentrations are (1) 4.0 mM CV, (2) 1.0 mM CV, and (3) 10.0 mM CV after rinsing only.

adsorbed layers the beam must pass through. Several independent trials for CV consistently resulted in the value of .023 for $2a_{ad}hc_{ad}$ which gives an area of $115.5 \times 10^{-16} \text{ cm}^2$ /molecule assuming the surface roughness is unity and a_{ad} is $8 \times 10^4 \text{ l mole}^{-1} \text{ cm}^{-1}$, which is the absorptivity in solution of CV at 530 nm.

The effective optical constants of a thin absorbing adsorbed film can be approximated from the absorbance measurements in a procedure analogous to that described in reference 2. Using these as initial guess vectors, A_{ad} values, as determined by extrapolation of absorbance measurements for 0 transmission, 72 parallel and 72 perpendicular polarization all at $\lambda=530 \text{ nm}$, were fed into an optical inversion program resulting in the converged optical constants being $n_{ad} = .8756$, $K_{ad} = 1.112$, and $h = 16.6 \text{ \AA}$. The exact equations using the space time average of E^2 in the adsorbed layer, which deviates about 8% through the film, yields a sensitivity factor of 3.14 for the adsorbed layer and 2.56 for parallel and perpendicular polarization, respectively. The presence of this adsorbed layer decreases b_{off} by a factor of .84 while b_{off} is enhanced to 1.05 times its value at the glass-solution interface. Following the previous assumptions as for transmission, Γ_{ad} is now $2.5 \times 10^{-10} \text{ mole cm}^{-2}$ giving the area per adsorbed molecule of $66.4 \times 10^{-16} \text{ cm}^2$. The surface roughness is probably something other than unity and plays a more important role in internal reflection measurements than for transmission.

Analogous absorbance-concentration curves to Figure

5 but using a thin gold film are presented in Figure 7. Again extrapolation to $c=0$ gives the absorbance contribution due to the adsorbed layer which is negligible for Eosin B as expected. The perpendicular component is suppressed with the addition of this thin gold film while the parallel component appears slightly reduced. Theoretical absorbance values calculated from the exact equations for the space time average of E inside the adsorbed layer using the optical constants as determined by EWS indicate CV adsorbs differently on gold than on glass. The ratio of EWSF to EWS for both polarizations indicate that only 0.6 of the layer which adsorbs onto the glass adsorbs onto the gold film. This is probably due to the gold film being more inert than the glass and different Au-CV bonds existing such that a lesser amount of dye adsorbs onto the film.

Table 1 is a comparison of the solution contributions with theoretical calculations and is illustrated by the ratios of the slopes taken from Figures 5 and 7. The discrepancies from calculated values are partly due to the changing index of the solution phase but mostly due to the deviations of absorptivity with changing concentration.

Conclusion

Evanescent wave spectroscopy has been shown to provide a new sensitive means of studying adsorbed species during electrochemical processes. An optically transparent thin evaporated gold film on a glass substrate served both as the optical plate for EWSF and the working

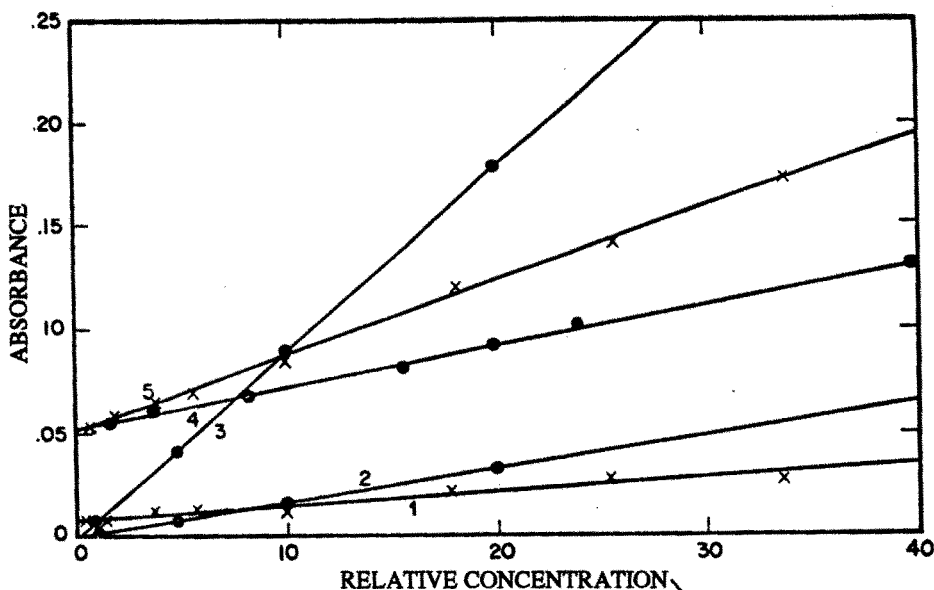


Figure 7. EWSF absorbance-concentration behavior per reflection at 72° using a 60 \AA gold film vacuum evaporated on a microscope slide. Solutions are (1) .75 mM CV, pH of 6.0, $\lambda=540 \text{ nm}$, and \perp polarization, (2) 5 gm of Eosin B per liter of pH 7.4 buffer, $\lambda=512 \text{ nm}$, and \perp polarization, (3) same as (2) except \parallel polarization, (4) similar to (1) except .4 mM CV and \parallel polarization, (5) same as (1) except \parallel polarization.

Table 1. Ratio of absorbance slopes for crystal violet and Eosin B in solution

Absorbance Ratios	Crystal Violet		Eosin B	
	Exp.	Calc.*	Exp.	Calc.
$\frac{EWSF_i}{EWS_i}$	1.32	1.30	1.45	1.42
$\frac{EWSF_l}{EWS_l}$.33	.35	.30	.25
$\frac{EWSF_l}{EWS_i}$.27	.23	.26	.22

*Calculation takes into account a 17 Å CV adsorbed layer with $n= .876$ and $k= 1.112$.

electrode in the electrochemical cell. In contrast to external reflectance and transmission, EWSF observations probe only the region near the electrode, typically one-tenth of the incident radiation wavelength. Hence, the presence or absence of absorbing adsorbed species even in highly absorbing electrolytes can be detected. Parameters were chosen where electroreflectance was negligible and adsorption-desorption preceded the redox process.

The possibilities of EWSF in studying surface physics are limitless. Little has yet been done in the UV or IR where most biological systems are of interest. Refinement of techniques and incorporation of more sophisticated recording devices would enable exact determination of adsorption rates in addition to catalysis effects and corre-

sponding redox systems.

References

1. Hansen, W.N. In *Advances in electrochemistry and electrochemical engineering* 9, (ed. P. Delahay and C.W. Tobias). John Wiley and Sons, New York, 1 (1983).
2. Behfrooz, M.R. Optical characterization of very thin films. *Iranian J. of Sci. and Tech.*, 1, 11, (1987).
3. Hansen, W.N. *Spectrochim. Acta*, 21, 815, (1985).
4. Behfrooz, M.R. and Woollam, J.A. Optical properties of thin films of methylene-blue and crystal-violet organic dyes using variable angle spectroscopic ellipsometry. *Applied Physics Communications*, U.S.A. 11, (2&3), 117-126, (1992).
5. Rabinwitch, E. and Epstein, L.F. *J. Amer. Chem. Soc.*, 63, 69, (1991).